(–)-Epigallocatechin-3-*O*-gallate upregulates the expression levels of miR-6757-3p, a suppressor of fibrosis-related gene expression, in extracellular vesicles derived from human umbilical vein endothelial cells

MOTOKI MURATA[1,2*], YUKI MARUGAME[1*], MAI MOROZUMI[1], KYOSUKE MURATA[1], MOTOFUMI KUMAZOE[1], YOSHINORI FUJIMURA[1] and HIROFUMI TACHIBANA[1]

[1]Division of Applied Biological Chemistry, Department of Bioscience and Biotechnology, Faculty of Agriculture, Kyushu University, Fukuoka 819-0395; [2]Advanced Research Support Center (ADRES), Ehime University, Matsuyama, Ehime 790-8566, Japan

Received August 16, 2022; Accepted January 3, 2023

DOI: 10.3892/br.2023.1601

Abstract. As pulmonary fibrosis (PF), a severe interstitial pulmonary disease, has such a poor prognosis, the development of prevention and treatment methods is imperative. (–)-Epigallocatechin-3-*O*-gallate (EGCG), one of the major catechins in green tea, exerts an antifibrotic effect, although its mechanism remains unclear. Recently, it has been reported that microRNAs (miRNAs or miRs) transported by extracellular vesicles (EVs) from vascular endothelial cells (VECs) are involved in PF. In the present study, the effects of EGCG on the expression of miRNAs in EVs derived from human umbilical vein endothelial cells (HUVECs) were assessed and miRNAs with antifibrotic activity were identified. miRNA microarray analysis revealed that EGCG modulated the expression levels of 31 miRNAs (a total of 27 miRNAs were upregulated, and 4 miRNAs were downregulated.) in EVs from HUVECs. Furthermore, TargetScan analysis indicated that miR-6757-3p in particular, which exhibited the highest degree of change, may target transforming growth factor-β (TGF-β) receptor 1 (TGFBR1). To evaluate the effects of miR-6757-3p on TGFBR1 expression, human fetal lung fibroblasts (HFL-1) were transfected with an miR-6757-3p mimic. The results demonstrated that the miR-6757-3p mimic downregulated the expression of TGFBR1 as well the expression levels of fibrosis-related genes including fibronectin and α-smooth muscle actin in TGF-β-treated HFL-1 cells. In summary, EGCG upregulated the expression levels of miR-6757-3p, which may target TGFBR1 and downregulate fibrosis-related genes, in EVs derived from VECs.

Correspondence to: Professor Hirofumi Tachibana, Division of Applied Biological Chemistry, Department of Bioscience and Biotechnology, Faculty of Agriculture, Kyushu University, 744 Motooka, Nishi-ku, Fukuoka 819-0395, Japan
E-mail: tatibana@agr.kyushu-u.ac.jp

*Contributed equally

Abbreviations: α-SMA, α-smooth muscle actin; EGCG, (–)-epigallocatechin-3-O-gallate; EVs, extracellular vesicles; HFL-1, human fetal lung fibroblasts; HUVECs, human umbilical vein endothelial cells; miRNA, microRNA; PF, pulmonary fibrosis; RT-qPCR, reverse transcription-quantitative polymerase chain reaction; TGF-β, transforming growth factor-β; TGFBR1, transforming growth factor-β receptor 1; VECs, vascular endothelial cells; 67LR, 67-kDa laminin receptor

Key words: (–)-epigallocatechin-3-O-gallate, fibrosis, microRNA, extracellular vesicles, transforming growth factor-β

Introduction

Pulmonary fibrosis (PF) is a serious interstitial lung disease characterized by an abnormal accumulation of the extracellular matrix and destruction of the architecture of the lungs (1). PF is classified into the most common idiopathic PF and other types caused by factors such as genetic mutations or exposure to toxic chemicals or radiation (2,3). The onset and progression of PF is mediated by the activation of pulmonary epithelial cells, the release of cytokines and growth factors, the proliferation and activation of myofibroblasts, and the abnormal deposition and transformation of the extracellular matrix (3). Current treatments for PF include antifibrotic agents, corticosteroids, and immunosuppressive drugs, but the prognosis for PF remains poor (4,5). The development of preventive and therapeutic strategies for PF is therefore an urgent priority.

Plants are rich in polyphenols, which are non-nutritive secondary metabolites; thus, humans consume polyphenols in their diet (6). The intake of these polyphenols has been reported to prevent various diseases such as diabetes and cardiovascular disease (7,8). Green tea (*Camellia sinensis*, Theaceae) is commonly consumed worldwide and has several dietary benefits such as antioxidative, anti-inflammatory, antiobesity, and antifibrotic effects (9-12). (–)-Epigallocatechin-3-*O*-gallate

(EGCG) is the most abundant and active compound in green tea and has been proven to have anticancer, anti-inflammatory, vascular-protective, and antifibrotic effects (13-17). Previous studies have reported that EGCG suppresses the accumulation of pulmonary hydroxyproline and bleomycin-induced pulmonary fibrosis (18,19), although the mechanism of the antifibrotic effect of EGCG remains unclear.

microRNAs (miRNAs or miRs) are a class of small, noncoding RNAs that bind directly to mRNA and regulate gene expression (18), thereby playing key roles in biological processes such as cell proliferation, metabolism, inflammation, and fibrosis (19-22). Furthermore, miRNAs have been shown to be involved in cell-to-cell communication by transferring from donor cells to recipient cells via extracellular vesicles (EVs) such as exosomes (23). In PF, miRNA let-7d, an exosomal miRNA derived from vascular endothelial cells (VECs), has been reported to regulate fibrosis by modulating the TGF-β signaling pathway (24). In previous studies, it has been reported that plant components such as polyphenols and miRNAs are involved in miRNA-mediated gene regulation in mice and humans (25-27). For example, polyphenol extracts from *Hibiscus sabdariffa* were shown to regulate the expression of miR-103, miR-107, and miR-122 and suppress fatty liver disease in hyperlipidemic mice (25). Plant miR-171 modulated G protein subunit α 12 signaling, including mechanistic target of rapamycin, in human embryonic kidney, 293 cells (26). In a clinical study, grape extract containing resveratrol increased the expression of miR-21, miR-181b, miR-663, and miR-30c and decreased inflammatory cytokine levels (27).

In the present study, it was hypothesized that EGCG exerts its antifibrotic effect via miRNAs contained in EVs from VECs, and EVs derived from human umbilical vein endothelial cells (HUVECs) were used to test this hypothesis. In addition, miRNAs with antifibrotic effects among the EGCG-altered miRNAs were identified and their influence on the expression of fibrosis-related genes was evaluated.

Materials and methods

Chemicals and materials. EGCG was purchased from Sigma-Aldrich; Merck KGaA, and recombinant human TGF-β1 was obtained from Bio-Techne. Optima™ MAX-XP Ultracentrifuge, MLS-50 rotor, and Ultra-Clear centrifuge tubes were purchased from Beckman Coulter, Inc. miRNA mimic Negative Control, mimic #1 (cat. no. SMC-2003) and miR-6757-3p mimic (5'-AACACUGGCCUUGCUAUCCC CA-3'; cat. no. SMM-003-MI0022602) were obtained from Bioneer Corporation. miR-6757-3p (cat. no. 339306; GeneGlobe ID YP02107562) and U6 primer (cat. no. 339306; GeneGlobe ID YP00203907) were purchased from Qiagen GmbH.

Cell culture. HUVECs (product no. KE-4109) were purchased from Kurabo Bio-Medical Department; Kurabo Industries, Ltd. and maintained with endothelial growth medium 2 (EGM-2; Lonza Group, Ltd.) containing 10% fetal bovine serum (FBS; Sigma-Aldrich; Merck KGaA). Human fetal lung fibroblasts (HFL-1; JCRB no. IFO50074) were obtained from the Japanese Collection of Research Bioresources Cell Bank and cultured in Dulbecco's modified Eagle's medium (DMEM; FUJIFILM Wako Pure Chemical Corporation) supplemented with 10% FBS. These cells were incubated at 37˚C with 5% CO_2 in a humidified chamber.

Isolation of EVs (ultracentrifugation). HUVECs were preincubated in 10% FBS/EGM-2 for 24 h and then incubated in 1% bovine serum albumin (BSA)/Medium 199 (M199) obtained respectively, from Roche Diagnostics and Gibco; Thermo Fisher Scientific, Inc. After 2 h, HUVECs were treated with 5 μM EGCG. The dose of EGCG was determined according to previous studies (28,29). Following a 24-h incubation with M199, the supernatant was collected. Debris and dead cells in the collected supernatant of the culture were removed by centrifugation at 2,000 x g for 10 min at 4˚C, and then filtrated through a 0.2-μm filter (Sartorius Stedim Biotech GmbH). Next, the supernatant of the culture was ultracentrifuged at 210,000 x g for 38 min at 4˚C. After the supernatant was aspirated, the EV pellets were washed with PBS and ultracentrifuged (210,000 x g for 38 min at 4˚C). Following a second aspiration, the pellets were resuspended with PBS.

Western blotting. EVs were lysed in lysis buffer containing 50 mM Tris-HCl (pH 7.5), 50 mM sodium fluoride, 0.15 M NaCl, 1% Triton X-100, 1 mM EDTA, 30 mM sodium pyrophosphate, 1 mM phenyl-methanesulfonyl fluoride, and 2 mg/ml aprotinin. Protein concentrations were determined by bicinchoninic acid (BCA) assay. Laemmli sample buffer containing 0.1 M Tris-HCl buffer (pH 6.8), 1% SDS, 0.05% mercaptoethanol, 10% glycerol, and 0.001% bromophenol blue was added and boiled (95˚C, 5 min). Proteins (5 μg/lane) were separated by reducing 8% (weight/volume) polyacrylamide gel electrophoresis and electroblotted on nitrocellulose blotting membranes (Cytiva). The membranes were blocked for 1 h at room temperature in 0.1% Tween-20/Tris-buffered saline containing 1% bovine serum albumin (all from Nacalai Tesque, Inc.) and incubated overnight at 4˚C in the presence of anti-CD9 antibodies (1:100,000 dilution; cat. no. sc-9148; Santa Cruz Biotechnology, Inc.). After the membranes were washed and then incubated (25˚C, 1 h) with the appropriate HRP-conjugated goat anti-rabbit secondary antibody (1:10,000 dilution; cat. no. 12-348; EMD Millipore), the bands were visualized using TMA-6 chemiluminescence reagent (Lumigen, Inc.; Beckman Coulter, Inc.). The band images were obtained using FUSION Solo S (Vilber-Lourmat).

Microarray analysis. Microarray analysis on a 3D-Gene® Human miRNA Oligo chip ver. 21 (Toray Industries Inc.) was outsourced to Toray Industries, Inc. Briefly, RNA samples were extracted from EVs using miRNeasy mini kit (Qiagen GmbH). The RNA concentration was measured using NanoDrop1000 (Thermo Fisher Scientific, Inc.) and RNA fluorescence labeling was performed using a 3D-Gene® miRNA labeling kit (cat. no. TRT-XE211; Toray Industries Inc.). 3D-Gene® Scanner (Toray Industries Inc.) was used for scanning. Data analysis was performed as follows: The blank value (average of the C1 blank) was subtracted from the sample measurements and set to 0 if the value was <0. The fold change was calculated to be equal to the average of the EGCGs divided by the average of the control. miRNAs with two or more samples with a value of 0 were excluded from the analysis. Binding

Table I. Primer sequences.

Gene	Forward	Reverse
ACTB	5'-TGGCACCCAGCACAATGAA-3'	5'-CTAAGTCATAGTCCGCCTAGAAGCA-3'
α-SMA	5'-CCGACCGAATGCAGAAGGA-3'	5'-ACAGAGTATTTGCGCTCCGGA-3'
FIBRONECTIN	5'-GGAGAATTCAAGTGTGACCCTCA-3'	5'-TGCCACTGTTCTCCTACGTGG-3'
TGFBR1	5'-GACAACGTCAGGTTCTGGCTCA-3'	5'-CCGCCACTTTCCTCTCCAAACT-3'

α-SMA, α-smooth muscle actin; *TGFBR1*, transforming growth factor-β receptor 1.

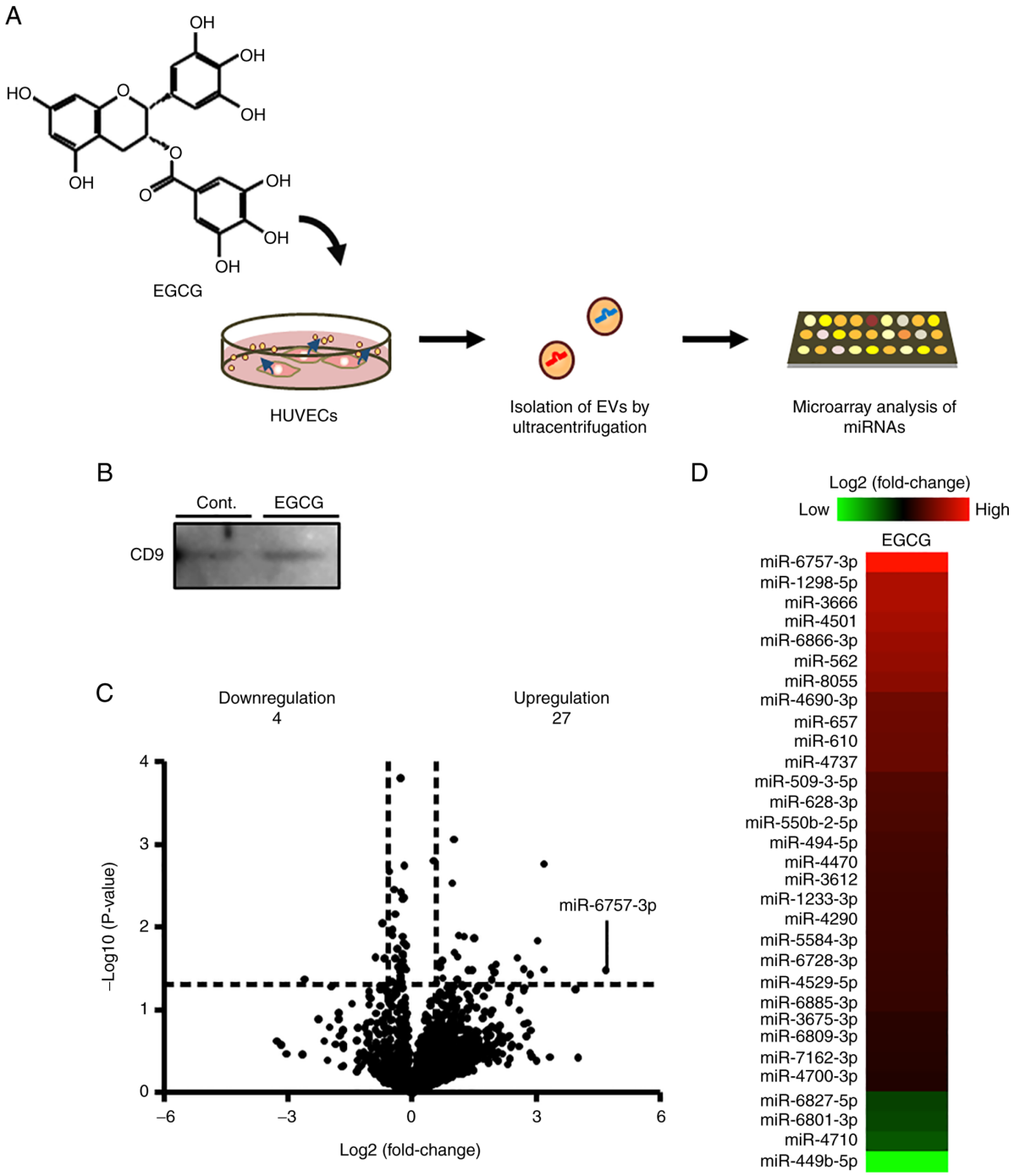

Figure 1. Effects of EGCG on the expression of miRNAs in EVs derived from HUVECs. (A) EVs were isolated from supernatants of EGCG-treated or untreated HUVECs by ultracentrifugation. (B) CD9 expression in EVs was measured by western blotting (n=1). Expression of miRNAs in EVs from HUVECs was assessed using miRNA microarray analysis (n=3). The results are shown in the (C) volcano plot and (D) heat map (fold change <0.67 or >1.5; P<0.05). EGCG, (–)-epigallocatechin-3-*O*-gallate; miRNA, microRNA; EVs, extracellular vesicles; HUVECs, human umbilical endothelial cells.

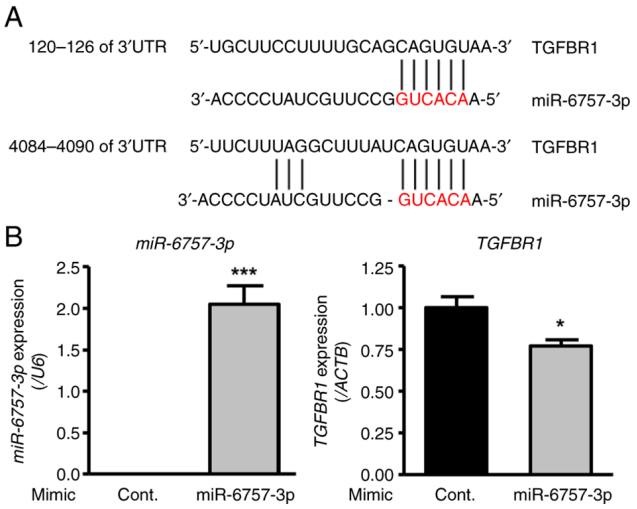

Figure 2. Effect of the miR-6757-3p mimic on the expression of TGFBR1. (A) TargetScan analysis was performed, and the binding sites of miR-6757-3p and TGFBR1 are shown. (B) HFL-1 cells were transfected with 20 nM of the miR-6757-3p mimic. The expression levels of miR-6757-3p and TGFBR1 were measured using reverse transcription-quantitative PCR. Data are presented as the mean ± SEM (n=4). *P<0.05 and ***P<0.001, determined using Student's t-test. miR-6757-3p, microRNA-6757-3p; TGFBR1, transforming growth factor-β receptor 1; Cont., control.

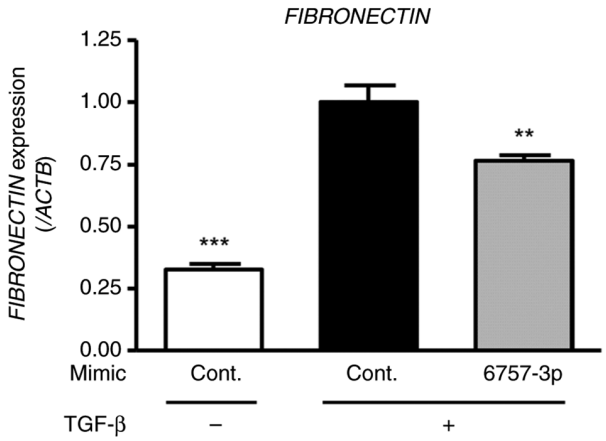

Figure 3. Suppressive effects of miR-6757-3p on fibronectin expression levels in TGF-β-treated HFL-1 cells. HFL-1 cells were transfected with 20 nM of the miR-6757-3p mimic and then treated with TGF-β to a final concentration of 5 ng/ml. The expression levels of fibronectin were assessed using reverse transcription-quantitative PCR. Data are presented as the mean ± SEM (n=4). **P<0.01 and ***P<0.001 vs. TGF-β + cont. mimic, determined using Dunnett's multiple comparison test. miR-6757-3p, microRNA-6757-3p; TGF-β, transforming growth factor-β; Cont., control.

sites of microRNA were predicted using TargetScan Release 8.0 (https://www.targetscan.org/vert_72/).

Transfection of miRNA mimics into HFL-1 cells. HFL-1 cells were cultured in 10% FBS/DMEM for 24 h. Each miRNA mimic was introduced into HFL-1 cells using Lipofectamine™ RNAiMAX (Invitrogen; Thermo Fisher Scientific, Inc.) as follows. The solution containing the mimics, RNAiMAX, and DMEM was mixed mildly by pipetting. After a subsequent incubation for 10 min at room temperature, the medium surrounding the HFL-1 cells was replaced with the mimic

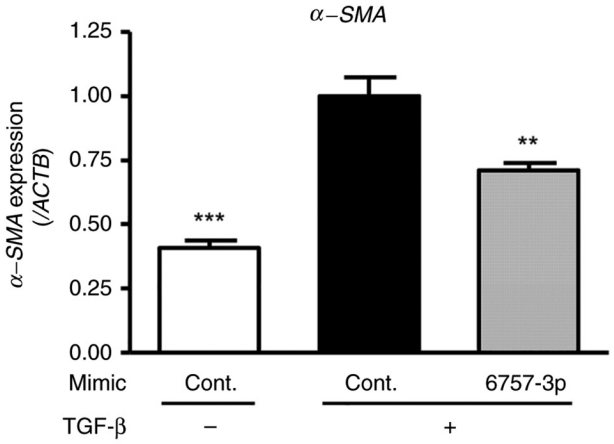

Figure 4. Suppressive effects of miR-6757-3p on α-SMA expression levels in TGF-β-treated HFL-1 cells. HFL-1 cells were transfected with 20 nM of the miR-6757-3p mimic and then treated with TGF-β to a final concentration of 5 ng/ml. The expression levels of α-SMA were assessed using reverse transcription-quantitative PCR. Data are presented as the mean ± SEM (n=4). **P<0.01 and ***P<0.001 vs. TGF-β + cont. mimic, determined using Dunnett's multiple comparison test. miR-6757-3p, microRNA-6757-3p; α-SMA, α-smooth muscle actin; TGF-β, transforming growth factor-β; Cont., control.

solution (37˚C, 5 h). The final concentration of the control or miR-6757-3p mimics was 20 nM. The concentration was determined according to a previous study (30). Subsequently, 5 h after transfection, HFL-1 cells were treated with 10% FBS/DMEM with or without TGF-β (the concentration of TGF-β was 5 ng/ml) for 48 h. Finally, HFL-1 cells were lysed using the TRI reagent® (Sigma-Aldrich; Merck KGaA).

Reverse transcription-quantitative polymerase chain reaction (RT-qPCR). RNA was extracted from HLF-1 cells using the TRI Reagent® (Molecular Research Center, Inc.). cDNA synthesis was performed using a PrimeScript RT Reagent Kit (Takara Bio, Inc.) or miRCURY LNA RT kit (Qiagen GmbH). cDNA of mRNA was mixed with SsoAdvanced Universal SYBR Green Supermix (Bio-Rad Laboratories, Inc.) and primers (Table I). cDNA of miRNA was mixed with miRCURY LNA SYBR Green Master Mix (Qiagen GmbH) and miR-6757-3p or U6 primers. Gene expression was assessed using CFX96™ or CFX384™ Real-Time PCR System and CFX Maestro version 3.1.1517.0823 software (Bio-Rad Laboratories, Inc.). The thermocycling protocol for mRNA consisted of an initial cycle at 95˚C for 3 min, followed by 50 cycles at 95˚C for 2 sec and 60˚C for 10 sec, and finally from 65˚C to 95˚C. The thermocycling protocol for miRNA consisted of an initial cycle at 95˚C for 10 min, followed by 50 cycles at 95˚C for 10 sec and 60˚C for 1 min, and finally 60˚C for 30 sec after increasing from 65˚C to 95˚C. mRNA expression was normalized to ACTB. miRNA expression was normalized to U6. Results are shown as relative values with the mean of the control or TGF-β + cont. mimic group set to 1 (except for miRNA data in Fig. 2B).

Statistical analysis. Microarray data (n=3) were analyzed using Student's t-tests and Microsoft Excel. The results in Figs. 2-4 (n=4) are presented as the mean ± standard error of the mean (SEM). The data were analyzed by a Student's unpaired t-test

Table II. Upregulated and downregulated miRNAs in extracellular vesicles of human umbilical vein endothelial cells after treatment with EGCG.

Upregulation			Downregulation		
miRNA[a]	Fold change[b]	P-value[c]	miRNA[a]	Fold change[b]	P-value[c]
miR-6757-3p	25.85	0.033	miR-449b-5p	0.17	0.043
miR-1298-5p	9.11	0.002	miR-4710	0.54	0.023
miR-3666	9.08	0.033	miR-6801-3p	0.61	0.009
miR-4501	8.20	0.015	miR-6827-5p	0.63	0.024
miR-6866-3p	7.20	0.037			
miR-562	6.52	0.032			
miR-8055	5.86	0.023			
miR-4690-3p	4.11	0.028			
miR-657	3.98	0.035			
miR-610	3.82	0.030			
miR-4737	3.79	0.043			
miR-509-3-5p	2.82	0.013			
miR-628-3p	2.73	0.033			
miR-550b-2-5p	2.58	0.033			
miR-494-5p	2.39	0.013			
miR-4470	2.32	0.050			
miR-3612	2.19	0.013			
miR-1233-3p	2.15	0.043			
miR-4290	2.14	0.023			
miR-5584-3p	2.12	0.042			
miR-6728-3p	2.02	0.020			
miR-4529-5p	2.02	0.001			
miR-6885-3p	1.96	0.003			
miR-3675-3p	1.67	0.041			
miR-6809-3p	1.65	0.025			
miR-7162-3p	1.59	0.030			
miR-4700-3p	1.50	0.047			

[a]miRNAs altered by EGCG (fold change <0.67 or >1.5; P<0.05). [b]Fold change=(average of EGCG)/(average of control). [c]Student's t-test. miRNA or miR, microRNA; EGCG, (−)-epigallocatechin-3-*O*-gallate.

(Fig. 2) or one-way ANOVA followed by Dunnett's multiple comparison test (Figs. 3 and 4, vs. TGF-β + cont. mimic) using GraphPad Prism 5.01 (GraphPad Software, Inc.). A value of P<0.05 was a considered to indicate a statistically significant difference.

Results

Effects of EGCG on the expression of miRNAs in EVs derived from HUVECs. Although EGCG exhibits antifibrotic activity, its mechanism is still unknown. Recently, miRNAs in EVs derived from VECs were reported to regulate fibrosis (24). In the present study, miRNA microarray analysis was performed to examine the regulatory effects of EGCG on the expression of miRNAs in EVs from HUVECs (Fig. 1A). Western blotting revealed the expression of CD9, an EV marker, which confirmed the successful isolation of EVs by ultracentrifugation (Fig. 1B). Microarray analysis revealed that EGCG upregulated 27 miRNAs and downregulated 4 miRNAs in EVs from HUVECs (Fig. 1C and D; Tables II and SI).

Effect of miR-6757-3p on the expression of transforming growth factor-β receptor 1 (TGFBR1), a candidate target gene. miRNAs with antifibrotic effects were investigated. Among the miRNAs whose expression increased as a result of EGCG treatment, miR-6757-3p was focused on because it showed the highest fold change. TargetScan analysis indicated that miR-6757-3p can target TGFBR1 (position 120-126 or 4084-4090 of 3'UTR) (Fig. 2A). In addition, TargetScan analysis of the 26 miRNAs (excluding miR-6757-3p) that were increased in expression by EGCG treatment revealed that nine miRNAs (miR-3666, miR-4501, miR-657, miR-509-3-5p, miR-3612, miR-6728-3p, miR-4529-5p, miR-6885-3p, miR-6809-3p) could target TGFBR1 (data not shown). The TGFBR1 signaling pathway controls collagen deposition and fibrosis (31). To investigate whether miR-6757-3p suppresses

TGFBR1 expression, miR-6757-3p mimics were transfected into HFL-1 cells. As a result, the transfection of miR-6757-3p mimics upregulated the expression of miR-6757-3p and downregulated the expression level of TGFBR1 (Fig. 2B). These findings indicated that miR-6757-3p is able to suppress TGFBR1.

Effects of miR-6757-3p on the expression of fibrosis-related genes in TGF-β-treated HFL-1 cells. To evaluate the impact of miR-6757-3p on fibrosis-related gene expression, including fibronectin and α-smooth muscle actin (α-SMA), HFL-1 cells were transfected with miR-6757-3p mimics and treated with TGF-β (for a final concentration of 5 ng/ml) for 48 h. The results revealed that TGF-β treatment increased fibronectin and α-SMA expression in the HFL-1 cells. Furthermore, there was a significant difference between the TGF-β + cont. mimic groups and the TGF-β + miR-6757-3p mimic groups (Figs. 3 and 4). These results indicated that miR-6757-3p downregulated the expression of fibrosis-related genes by suppressing the expression of TGFBR1.

Discussion

In the present study, it was demonstrated that EGCG altered the expression of 31 miRNAs (a total of 27 miRNAs were upregulated, and 4 miRNAs were downregulated.) in EVs derived from HUVECs. These miRNAs may be involved in the physiological effects of EGCG. The results revealed that miR-6757-3p, which had the highest fold change ratio after EGCG treatment, decreased fibrosis-related gene expression in genes such as fibronectin and α-SMA in pulmonary fibroblasts. These findings indicated that miR-6757-3p may play a major role in activating the anti-PF effects of EGCG.

The present study indicated that miR-6757-3p may target TGFBR1 and downregulate the expression of fibrosis-related genes. TGFBR1 has been reported to regulate fibrosis through the TGF-β/Smad signaling pathway (32,33). In mice constitutively expressing active TGFBR1 in fibroblasts, promotion of Smad phosphorylation, myofibroblast differentiation, and fibrosis have been observed (34). Furthermore, a previous study has revealed that the deletion of TGFBR1 in fibroblasts suppresses fibrosis (35). TGFBR1 has attracted attention as a therapeutic target for fibrosis, and the TGFBR1 kinase inhibitor galunisertib (LY2157299) has reportedly exhibited liver regeneration-promoting and antifibrotic effects (36). The TGFBR1 signaling pathway has also been reported to be involved in myocardial and renal fibrosis as well as PF (31,37). Thus, miR-6757-3p could be a new preventive and therapeutic agent for the treatment of fibrosis in various organs.

In addition, miR-3666, whose expression increased via EGCG treatment in the present study, was reported to suppress hepatic steatosis by targeting PPARγ (38). A previous study reported that EGCG suppresses nonalcoholic fatty liver disease (39). Therefore, miR-3666 in HUVEC-derived EVs may be associated with the antihepatic steatosis effect of EGCG.

miRNAs in EVs play key roles in cell-to-cell communication. It has been demonstrated that EGCG may modulate intercellular communication via miRNAs in EVs derived from VECs and regulate various diseases, including PF. In addition, miRNAs contained in EVs have been reported to be correlated with the development of diseases and expected to be used as biomarkers (40). Considering the results observed using miR-6757-3p, it is hypothesized that it is feasible to use miR-6757-3p as a marker of the progression and prognosis of PF. Moreover, the 31 miRNAs whose expression was altered in the present study could be indicators of EGCG intake. Research into the effect of certain foods on the expression of miRNAs in EVs is not extensive to date, but given the results of the present study, future research is warranted.

The various biological properties of EGCG, including its anti-inflammatory and anticancer effects, are mediated through its 67-kDa laminin receptor (67LR) (41,42). EGCG has also been reported to regulate miRNA expression in melanoma cells via 67LR (43). Therefore, it is possible that 67LR is involved in the regulation of the 31 miRNAs whose expression was altered by EGCG treatment in the present study. However, further research is needed to investigate the potential association between 67LR and these 31 miRNAs.

In conclusion, EGCG altered the expression of various miRNAs including miR-6757-3p, which may target TGFBR1 and decrease fibrosis-related gene expression, in EVs derived from VECs. The results of the present study mark an important step toward a deeper understanding of the relationship between EGCG and functional miRNAs.

Acknowledgements

Not applicable.

Funding

The present study was supported in part by Grants-in-Aid for Scientific Research (KAKENHI) from the Japan Society for the Promotion of Science to HT (grant no. JP20H05683) and MMu (grant no. JP17H06936).

Availability of data and materials

The microarray data generated in the present study may be found in the GEO database under accession no. GSE217849 or at the following URL: https://www.ncbi.nlm.nih.gov/geo/query/acc.cgi?acc=GSE217849. The other data used and/or analyzed during the present study are available from the corresponding author upon reasonable request.

Authors' contributions

MMu, YM, MK, YF, and HT were involved in the conception and design of the study. MMu, YM, MMo, and KM performed the experiments. YM, MMo, KM, MK, and YF analyzed the data. MMu, YM and MK wrote the manuscript. MMu, YM, MK, and HT revised the manuscript. MMu and YM confirm the authenticity of all the raw data. All authors have read and approved the final manuscript.

Ethics approval and consent to participate

The HUVECs purchased from Kurabo Bio-Medical Department; Kurabo Industries, Ltd. are products that were

isolated from donated human tissue after obtaining permission for their use in research applications by informed consent or legal authorization.

Patient consent for publication

Not applicable.

Competing interests

The authors declare that they have no competing interests.

References

1. Wuyts WA, Agostini C, Antoniou KM, Bouros D, Chambers RC, Cottin V, Egan JJ, Lambrecht BN, Lories R, Parfrey H, *et al*: The pathogenesis of pulmonary fibrosis: a moving target. Eur Respir J 41: 1207-1218, 2013.
2. Thannickal VJ, Toews GB, White ES, Lynch JP III and Martinez FJ: Mechanisms of pulmonary fibrosis. Annu Rev Med 55: 395-417, 2004.
3. Richeldi L, Collard HR and Jones MG: Idiopathic pulmonary fibrosis. Lancet 389: 1941-1952, 2017.
4. Bouros D and Antoniou KM: Current and future therapeutic approaches in idiopathic pulmonary fibrosis. Eur Respir J 26: 693-703, 2005.
5. Luppi F, Cerri S, Beghè B, Fabbri LM and Richeldi L: Corticosteroid and immunomodulatory agents in idiopathic pulmonary fibrosis. Respir Med 98: 1035-1044, 2004.
6. Zamora-Ros R, Achaintre D, Rothwell JA, Rinaldi S, Assi N, Ferrari P, Leitzmann M, Boutron-Ruault MC, Fagherazzi G, Auffret A, *et al*: Urinary excretions of 34 dietary polyphenols and their associations with lifestyle factors in the EPIC cohort study. Sci Rep 6: 26905, 2016.
7. van Dam RM, Naidoo N and Landberg R: Dietary flavonoids and the development of type 2 diabetes and cardiovascular diseases: Review of recent findings. Curr Opin Lipidol 24: 25-33, 2013.
8. Wang X, Ouyang YY, Liu J and Zhao G: Flavonoid intake and risk of CVD: A systematic review and meta-analysis of prospective cohort studies. Br J Nutr 111: 1-11, 2014.
9. Xing L, Zhang H, Qi R, Tsao R and Mine Y: Recent advances in the understanding of the health benefits and molecular mechanisms associated with green tea polyphenols. J Agric Food Chem 67: 1029-1043, 2019.
10. Azambuja JH, Mancuso RI, Via FID, Torello CO and Saad STO: Protective effect of green tea and epigallocatechin-3-gallate in a LPS-induced systemic inflammation model. J Nutr Biochem 101: 108920, 2022.
11. Sae-tan S, Grove KA and Lambert JD: Weight control and prevention of metabolic syndrome by green tea. Pharmacol Res 64: 146-154, 2011.
12. Tsai CF, Hsu YW, Ting HC, Huang CF and Yen CC: The in vivo antioxidant and antifibrotic properties of green tea (*Camellia sinensis*, Theaceae). Food Chem 136: 1337-1344, 2013.
13. Wei H, Ge Q, Zhang LY, Xie J, Gan RH, Lu YG and Zheng DL: EGCG inhibits growth of tumoral lesions on lip and tongue of K-Ras transgenic mice through the Notch pathway. J Nutr Biochem 99: 108843, 2022.
14. Wang M, Zhong H, Zhang X, Huang X, Wang J, Li Z, Chen M and Xiao Z: EGCG promotes PRKCA expression to alleviate LPS-induced acute lung injury and inflammatory response. Sci Rep 11: 11014, 2021.
15. Meng J, Chen Y, Wang J, Qiu J, Chang C, Bi F, Wu X and Liu W: EGCG protects vascular endothelial cells from oxidative stress-induced damage by targeting the autophagy-dependent PI3K-AKT-mTOR pathway. Ann Transl Med 8: 200, 2020.
16. Sriram N, Kalayarasan S and Sudhandiran G: Epigallocatechin-3-gallate exhibits anti-fibrotic effect by attenuating bleomycin-induced glycoconjugates, lysosomal hydrolases and ultrastructural changes in rat model pulmonary fibrosis. Chem Biol Interact 180: 271-280, 2009.
17. Sriram N, Kalayarasan S and Sudhandiran G: Enhancement of antioxidant defense system by epigallocatechin-3-gallate during bleomycin induced experimental pulmonary fibrosis. Biol Pharm Bull 31: 1306-1311, 2008.
18. Cai Y, Yu X, Hu S and Yu J: A brief review on the mechanisms of miRNA regulation. Genomics Proteomics Bioinformatics 7: 147-154, 2009.
19. Shenoy A and Blelloch RH: Regulation of microRNA function in somatic stem cell proliferation and differentiation. Nat Rev Mol Cell Biol 15: 565-576, 2014.
20. Jordan SD, Krüger M, Willmes DM, Redemann N, Wunderlich FT, Brönneke HS, Merkwirth C, Kashkar H, Olkkonen VM, Böttger T, *et al*: Obesity-induced overexpression of miRNA-143 inhibits insulin-stimulated AKT activation and impairs glucose metabolism. Nat Cell Biol 13: 434-446, 2011.
21. Nejad C, Stunden HJ and Gantier MP: A guide to miRNAs in inflammation and innate immune responses. FEBS J 285: 3695-3716, 2018.
22. O'Reilly S: MicroRNAs in fibrosis: Opportunities and challenges. Arthritis Res Ther 18: 11, 2016.
23. Bayraktar R, Van Roosbroeck K and Calin GA: Cell-to-cell communication: microRNAs as hormones. Mol Oncol 11: 1673-1686, 2017.
24. Xie H, Gao YM, Zhang YC, Jia MW, Peng F, Meng QH and Wang YC: Low let-7d exosomes from pulmonary vascular endothelial cells drive lung pericyte fibrosis through the TGFβRI/FoxM1/Smad/β-catenin pathway. J Cell Mol Med 24: 13913-13926, 2020.
25. Joven J, Espinel E, Rull A, Aragonès G, Rodríguez-Gallego E, Camps J, Micol V, Herranz-López M, Menéndez JA, Borrás I, *et al*: Plant-derived polyphenols regulate expression of miRNA paralogs miR-103/107 and miR-122 and prevent diet-induced fatty liver disease in hyperlipidemic mice. Biochim Biophys Acta 1820: 894-899, 2012.
26. Gismondi A, Nanni V, Monteleone V, Colao C, Di Marco G and Canini A: Plant miR171 modulates mTOR pathway in HEK293 cells by targeting GNA12. Mol Biol Rep 48: 435-449, 2021.
27. Cione E, La Torre C, Cannataro R, Caroleo MC, Plastina P and Gallelli L: Quercetin, epigallocatechin gallate, curcumin, and resveratrol: From dietary sources to human MicroRNA modulation. Molecules 25: 63, 2019.
28. Ou HC, Song TY, Yeh YC, Huang CY, Yang SF, Chiu TH, Tsai KL, Chen KL, Wu YJ, Tsai CS, *et al*: EGCG protects against oxidized LDL-induced endothelial dysfunction by inhibiting LOX-1-mediated signaling. J Appl Physiol (1985) 108: 1745-1756, 2010.
29. Kanlaya R, Peerapen P, Nilnumkhum A, Plumworasawat S, Sueksakit K and Thongboonkerd V: Epigallocatechin-3-gallate prevents TGF-β1-induced epithelial-mesenchymal transition and fibrotic changes of renal cells via GSK-3β/β-catenin/Snail1 and Nrf2 pathways. J Nutr Biochem 76: 108266, 2020.
30. Marugame Y, Takeshita N, Yamada S, Yoshitomi R, Kumazoe M, Fujimura Y and Tachibana H: Sesame lignans upregulate glutathione S-transferase expression and downregulate microRNA-669c-3p. Biosci Microbiota Food Health 41: 66-72, 2022.
31. Tan Z, Jiang X, Zhou W, Deng B, Cai M, Deng S, Xu Y, Ding W, Chen G, Chen R, *et al*: Taohong siwu decoction attenuates myocardial fibrosis by inhibiting fibrosis proliferation and collagen deposition via TGFBR1 signaling pathway. J Ethnopharmacol 270: 113838, 2021.
32. Xu Z, He B, Jiang Y, Zhang M, Tian Y, Zhou N, Zhou Y, Chen M, Tang M, Gao J and Peng F: Igf2bp2 knockdown improves CCl_4-induced liver fibrosis and TGF-β-activated mouse hepatic stellate cells by regulating Tgfbr1. Int Immunopharmacol 110: 108987, 2022.
33. Schnaper HW, Hayashida T and Poncelet AC: It's a Smad world: Regulation of TGF-beta signaling in the kidney. J Am Soc Nephrol 13: 1126-1128, 2002.
34. Sonnylal S, Denton CP, Zheng B, Keene DR, He R, Adams HP, Vanpelt CS, Geng YJ, Deng JM, Behringer RR and de Crombrugghe B: Postnatal induction of transforming growth factor beta signaling in fibroblasts of mice recapitulates clinical, histologic, and biochemical features of scleroderma. Arthritis Rheum 56: 334-344, 2007.
35. Khalil H, Kanisicak O, Prasad V, Correll RN, Fu X, Schips T, Vagnozzi RJ, Liu R, Huynh T, Lee SJ, *et al*: Fibroblast-specific TGF-β-Smad2/3 signaling underlies cardiac fibrosis. J Clin Invest 127: 3770-3783, 2017.
36. Masuda A, Nakamura T, Abe M, Iwamoto H, Sakaue T, Tanaka T, Suzuki H, Koga H and Torimura T: Promotion of liver regeneration and anti-fibrotic effects of the TGF-β receptor kinase inhibitor galunisertib in CCl4-treated mice. Int J Mol Med 46: 427-438, 2020.

37. Li J, Yue S, Fang J, Zeng J, Chen S, Tian J, Nie S, Liu X and Ding H: MicroRNA-10a/b inhibit TGF-β/Smad-induced renal fibrosis by targeting TGF-β receptor 1 in diabetic kidney disease. Mol Ther Nucleic Acids 28: 488-499, 2022.
38. Mittal S, Inamdar S, Acharya J, Pekhale K, Kalamkar S, Boppana R and Ghaskadbi S: miR-3666 inhibits development of hepatic steatosis by negatively regulating PPARγ. Biochim Biophys Acta Mol Cell Biol Lipids 1865: 158777, 2020.
39. Naito Y, Ushiroda C, Mizushima K, Inoue R, Yasukawa Z, Abe A and Takagi T: Epigallocatechin-3-gallate (EGCG) attenuates non-alcoholic fatty liver disease via modulating the interaction between gut microbiota and bile acids. J Clin Biochem Nutr 67: 2-9, 2020.
40. Salehi M and Sharifi M: Exosomal miRNAs as novel cancer biomarkers: Challenges and opportunities. J Cell Physiol 233: 6370-6380, 2018.
41. Byun EB, Kim WS, Sung NY and Byun EH: Epigallocatechin-3-gallate regulates anti-inflammatory action through 67-kDa laminin receptor-mediated tollip signaling induction in lipopolysaccharide-stimulated human intestinal epithelial cells. Cell Physiol Biochem 46: 2072-2081, 2018.
42. Tachibana H, Koga K, Fujimura Y and Yamada K: A receptor for green tea polyphenol EGCG. Nat Struct Mol Biol 11: 380-381, 2004.
43. Yamada S, Tsukamoto S, Huang Y, Makio A, Kumazoe M, Yamashita S and Tachibana H: Epigallocatechin-3-O-gallate up-regulates microRNA-let-7b expression by activating 67-kDa laminin receptor signaling in melanoma cells. Sci Rep 6: 19225, 2016.